17th World Conference on Earthquake Engineering, 17WCEE
Sendai, Japan - September 13th to 18th 2020

EFFECTS AND DYNAMIC CHARACTERISTICS OF THE CORE-SUSPENDED ISOLATION SYSTEM

Y. Nakamura[(1)], K. Okada[(2)]

[(1)] *Professor, Dept. of Architectural Design, Shimane University, yutaka.nakamura@riko.shimane-u.ac.jp*
[(2)] *Senior Research Engineer, Institute of Technology, Shimizu Corporation, okka@shimz.co.jp*

Abstract

The seismic isolation mechanism of the core-suspended isolation (CSI) system comprises a double layer of inclined rubber bearings installed on top of a reinforced core structure. A multi-level structure is then suspended from a hat truss or umbrella girder constructed on the seismic isolation mechanism. The first building to use the CSI system was the Safety and Security Center in Tokyo, Japan, whose structural health monitoring system has detected and recorded 231 earthquake motions since 2006, including the 2011 Tohoku Pacific Earthquake (2011-TPE). The present study estimates the dynamic characteristics of this CSI-equipped building in earthquakes, and the effects of the CSI system are revealed via the observed earthquake records. The temporal changes of the fundamental period and damping factor are estimated from the 2011-TPE; the fundamental period increases with the deformation of the isolation level, whereas the fundamental damping factor is only related weakly to that deformation. The 231 observed earthquake records reveal that the CSI system performs seismic isolation by reducing the response acceleration of the suspended structure by roughly a half for peak ground accelerations exceeding 30 cm/s^2. Daily microtremor observations are used to diagnose earthquake damage; the fundamental frequencies in each direction remain almost constant and were not changed by the 2011-TPE.

Keywords: core-suspended isolation, structural health monitoring, 2011 Tohoku Pacific Earthquake

1. Introduction

The core-suspended isolation (CSI) system has been developed as an utterly new type of seismic isolation (SI) system [1, 2]. Unlike a conventional SI system, the isolation level of the CSI system is located at the top of the structure. The CSI system comprises a reinforced concrete core on top of which is installed an SI mechanism comprising a double layer of inclined rubber bearings to create a pendulum isolation mechanism. A multi-level structure is then suspended from a hat truss or umbrella girder constructed on the SI mechanism. The first CSI-equipped building was the Safety and Security Center in Tokyo, Japan (Fig. 1).

The seismic response of a building can be observed by means of various vibrometers, and the dynamic characteristics of the structure can be evaluated through system identification techniques [3-18]. Structural health monitoring (SHM) is a technology for examining structures physically by using installed sensors and a data acquisition/transmission system [19-21]. SHM can examine the physical condition of a structure under normal conditions and then diagnose any damage or changes due to an earthquake. SHM is quite useful for determining whether an affected structure can be used as it is, or how serious the damage is immediately after an earthquake. In addition, SHM can show how earthquake-proof performance is achieved by monitoring the physical status of the structure directly. The effects of SI systems have been recognized widely through the SHM of SI buildings, and the dynamic characteristics (e.g., fundamental frequency, damping factor) of SI buildings have been evaluated by means of SHM [22-24].

The SHM system of this first CSI building (hereinafter referred to simply as the CSI building) has detected and recorded 231 earthquake motions since 2006, including the 2011 Tohoku Pacific Earthquake (2011-TPE). The SHM system has also been collecting a 2-min microtremor trace at midnight each day. In the present study, the dynamic characteristics of the CSI building in earthquakes are estimated, and the effects of the CSI system are revealed via the observed earthquake records. Earthquake damage is diagnosed based on changes in the normal dynamic characteristics as revealed by the daily microtremor observations.

2. Building equipped with core-suspended isolation

The present CSI building is shown in Fig. 1 and the design details are given in Table 1. The building's SI mechanism comprises two layers each of four inclined rubber bearings installed at the top of a reinforced concrete core, from which three floors of office structure are suspended by high-strength steel rods [1, 2].

Fluid dampers as shown in Fig. 2 are installed between the core shaft and the suspended office structure at the second floor and rooftop levels. These dampers use a safety locking mechanism that is normally locked to brace the office structure against wind loads but that is released automatically in the event of an earthquake when the ground motion exceeds a threshold value. The latter is set as 5 cm/s^2 and 8 cm/s^2 RMS over 1 s in the horizontal and vertical directions, respectively.

(a) Photograph (left) and perspective drawing (right) of first CSI-equipped building

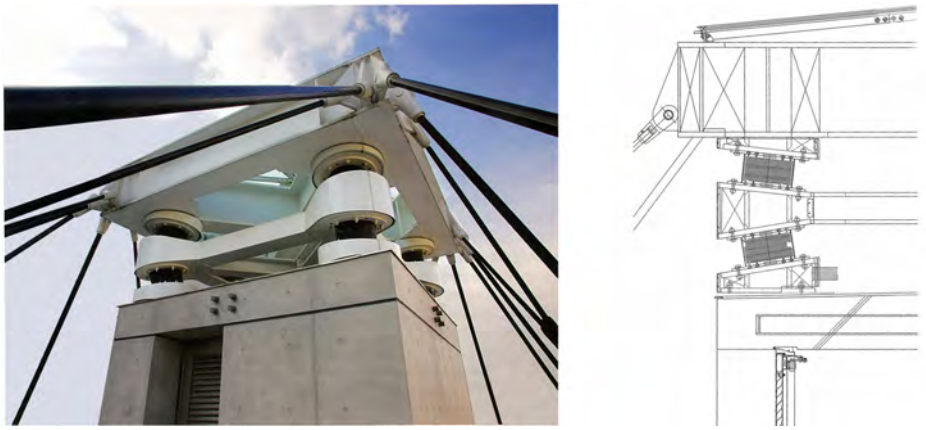

(b) Pendulum seismic isolation (SI) mechanism comprising two layers each of four inclined rubber bearings

Fig. 1 – First CSI building: the Safety and Security Center [2]

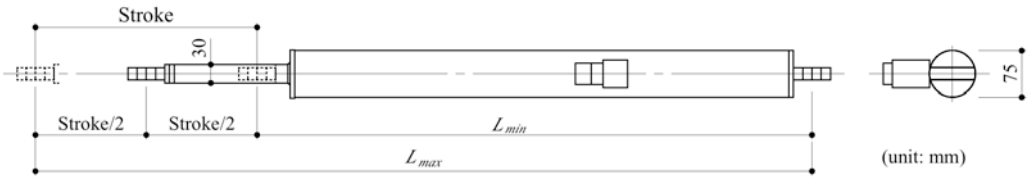

Maximum force [kN]	Limiting speed [m/s]	L_{min} [mm]	L_{max} [mm]	Stroke [mm]	Damping coefficient [kN s/m]	Lock force [kN]
50	1.0	1480	2200	720	50	50

Fig. 2 – Fluid damper with safety locking mechanism [2]

Table 1 – Details of Safety and Security Center [2, 22]

Floor area	Total: 213.65 m^2; first floor: 9.05 m^2; second-to-fourth floors: 66.15 m^2; penthouse: 6.15 m^2
Height	Total: 18.75 m; first floor: 4.15 m; second-to-fourth floors: 3.0 m
Core shaft	Reinforced concrete wall; 200-mm thick; 400-mm clearance joint
Suspended structure	Total weight: 180 ton; steel rod column 42-mm diameter
Rubber bearings	Two layers each of four inclined rubber bearings Diameter: 300 mm; inner steel shims: 1.2 mm × 45; rubber layers: 2.1 mm × 46; S1 = 35.7; S2 = 3.11; G = 0.29 MPa; horizontal stiffness = 215 kN/m Allowable horizontal deformation: 155 mm
Tilt angles	Lower layer: $\phi_1 = 9.9°$; upper layer: $\phi_2 = 6.6°$
Fluid dampers	Two dampers at second floor and four at rooftop level in X and Y directions
First-mode periods	5.08 s in X direction; 5.14 s in Y direction (design values)

3. Structural Health Monitoring in CSI Building

An SHM system was implemented in the CSI building to detect the seismic performance [20]. Fig. 3 shows the sensor arrangements (seven accelerometers, two displacement meters, and one wind anemometer), and a block diagram of the SHM system in the building. This system detects and records seismic vibrations when the observed acceleration of any accelerometer in any direction exceeds 3 cm/s^2 RMS for more than 1 s. When the control system receives the observed data from the sensors, the information display indicates an earthquake occurrence, and the fluid dampers are unlocked if the ground motion exceeds the threshold value.

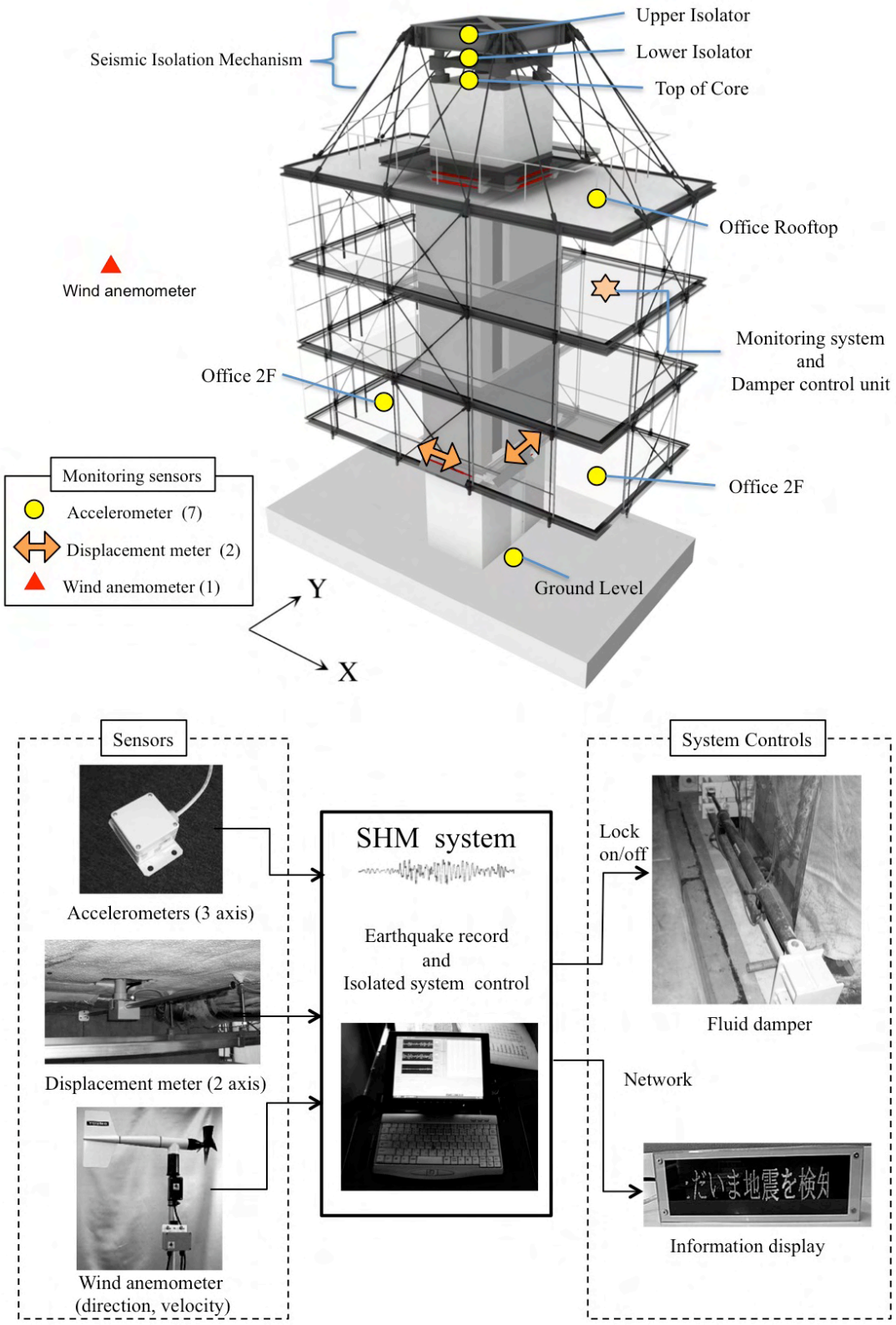

Fig. 3 – Structural health monitoring (SHM) system installed in CSI building [20]

4. Response of CSI Building to 2011 Tohoku Pacific Earthquake

4.1 Effects of 2011 Tohoku Pacific Earthquake on CSI System

The maximum acceleration responses of the Safety and Security Center when subjected to the 2011-TPE are shown in Fig. 4. Although the acceleration responses were amplified at the top of the core structure, the CSI system reduced them: compared to those on the ground, the maximum accelerations on the floors in the hung structure were reduced to about half in the X direction and to about one third in the Y direction.

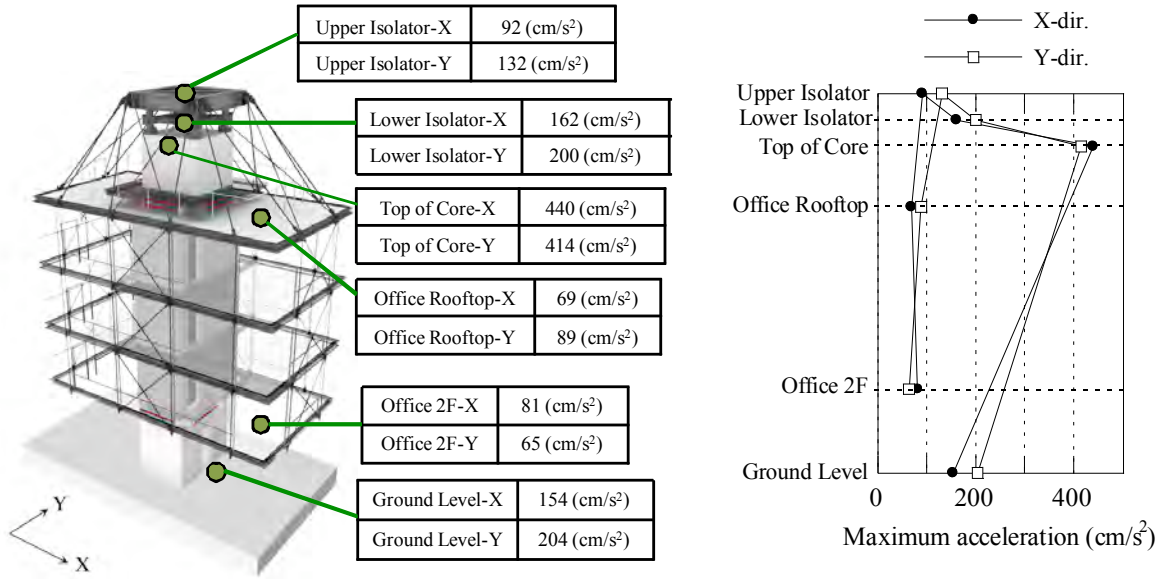

Fig. 4 – Maximum responses of CSI building [22]

4.2 Dynamic Characteristics of CSI System from 2011 Tohoku Pacific Earthquake

The dynamic characteristics of the building, namely the fundamental natural period and damping, were estimated from the 2011-TPE. An auto-regressive exogenous input (ARX) model [7, 11, 12, 16, 17] was applied to the observed acceleration waves by assigning the wave on the ground level as the input and the two waves on the office rooftop and on the office second floor as two outputs in each horizontal direction.

Fig. 5 and Fig. 6 show how the dynamic characteristics of the building vary in the X and Y directions, respectively. Fig. 5(a) and Fig. 6(a) show the deformation wave of the isolation level in each horizontal direction, D_x or D_y, which was obtained from the difference between the double-integrated acceleration wave of the upper isolator and that of the top of core. The locking mechanism of the fluid damper (Fig. 2) was released automatically at the time of 45.17 s.

Fig. 5(b) and (c) show the temporal changes of the estimated fundamental period T_{1x} and damping factor h_{1x}, respectively, in the X direction for every 10-s duration. Fig. 5(d) and (e) show the relationship between D_x and T_{1x} and that between D_x and h_{1x}, respectively. In the same way, Fig. 6(b) and (c) show the temporal changes of the estimated fundamental period T_{1y} and damping factor h_{1y}, respectively, in the Y direction for every 10-s duration, and Fig. 6(d) and (e) show the relationship between D_y and T_{1y} and that between D_y and h_{1y}, respectively.

The overall values of T_{1x}, T_{1y}, h_{1x}, and h_{1y} evaluated from the total observed records are presented in Fig. 5(b) and (c) and Fig. 6(b) and (c). Fig. 5(d) and Fig. 6(d) indicate that T_{1x} and T_{1y} increase with D_x and D_y, respectively, while h_{1x} and h_{1y} vary widely and are related only weakly to D_x and D_y as indicated in Fig. 5(e) and Fig. 6(e).

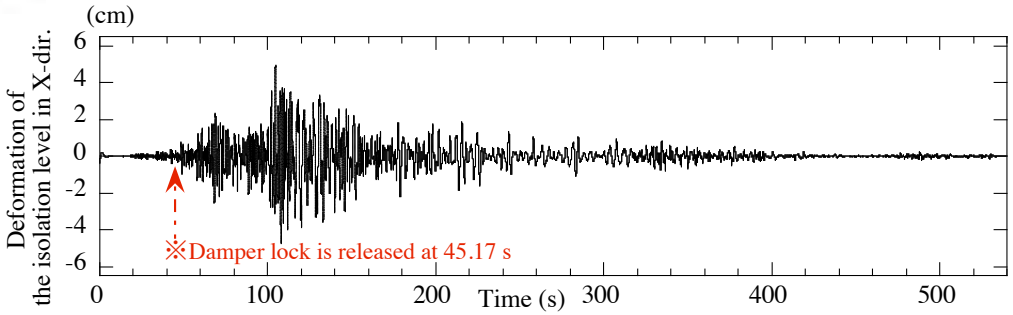

(a) Calculated deformation waves of the isolation level in X-dir.

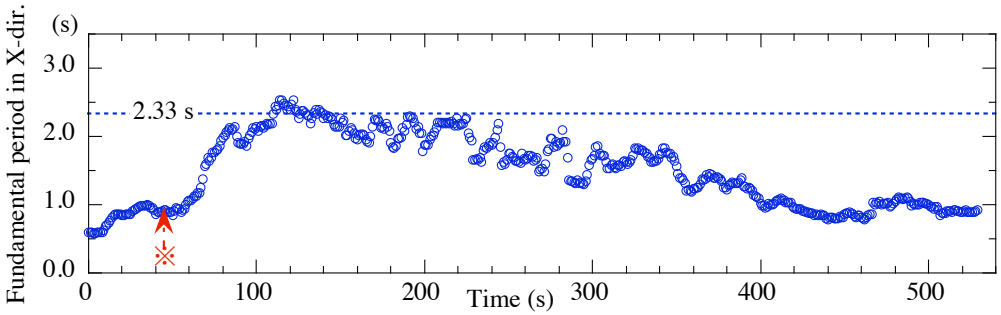

(b) Estimated fundamental period in X-dir. for every 10-s duration

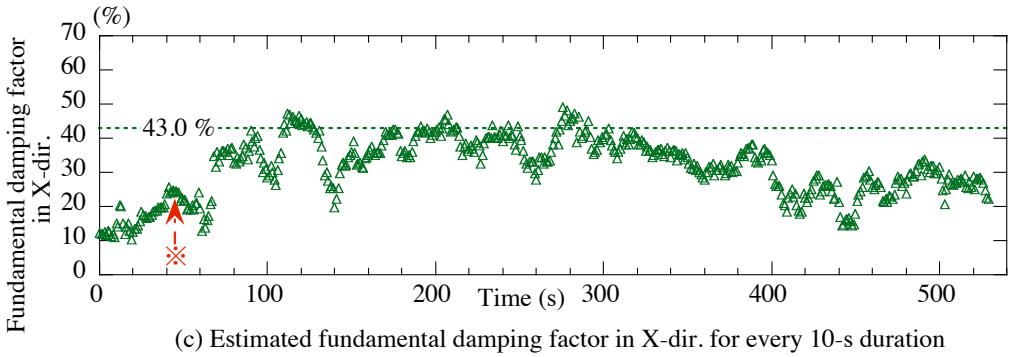

(c) Estimated fundamental damping factor in X-dir. for every 10-s duration

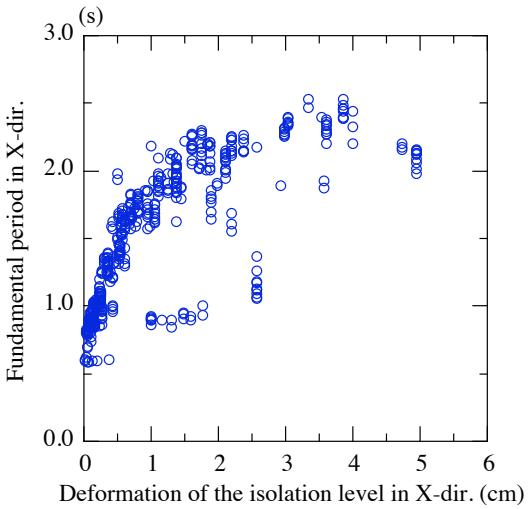

(d) Relationship between deformation of the isolation level and fundamental period in X-dir.

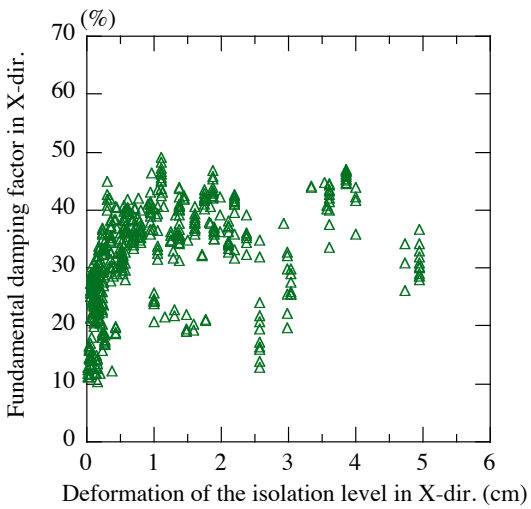

(e) Relationship between deformation of the isolation level and fundamental damping factor in X-dir.

Fig. 5 – Variations of dynamic characteristics of CSI building in X direction

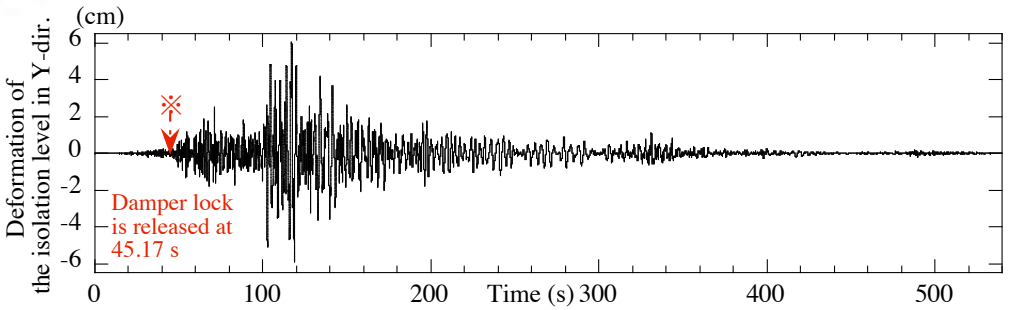

(a) Calculated deformation waves of the isolation level in Y-dir.

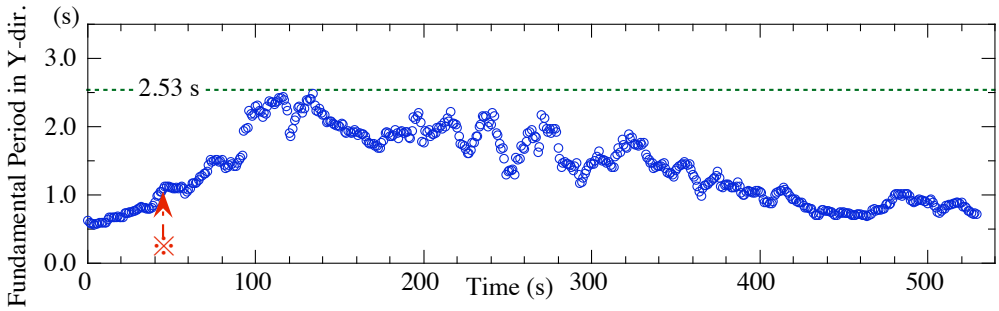

(b) Estimated fundamental period in Y-dir. for every 10-s duration

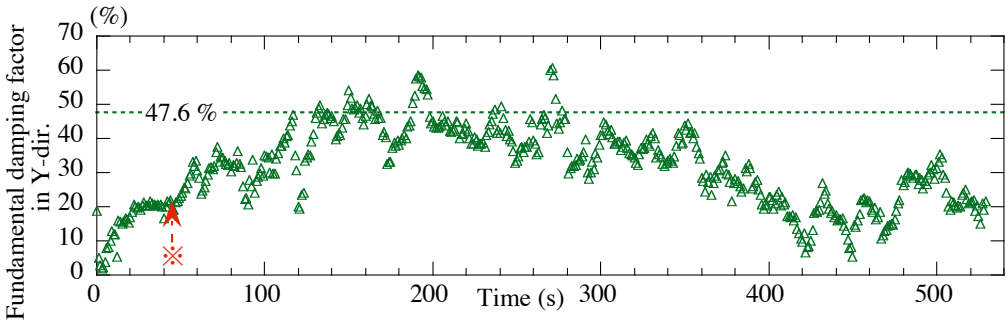

(c) Estimated fundamental damping factor in Y-dir. for every 10-s duration

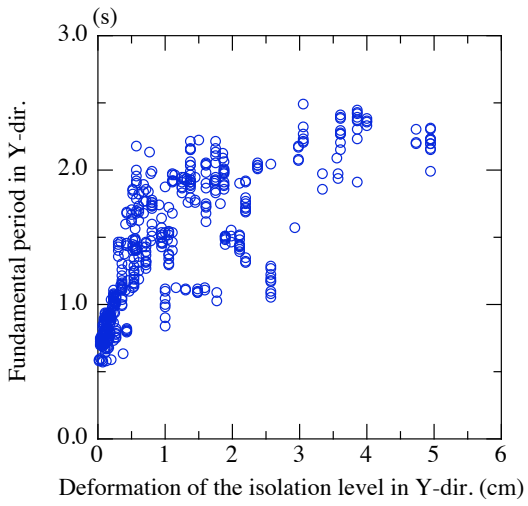

(d) Relationship between deformation of the isolation level and fundamental period in Y-dir.

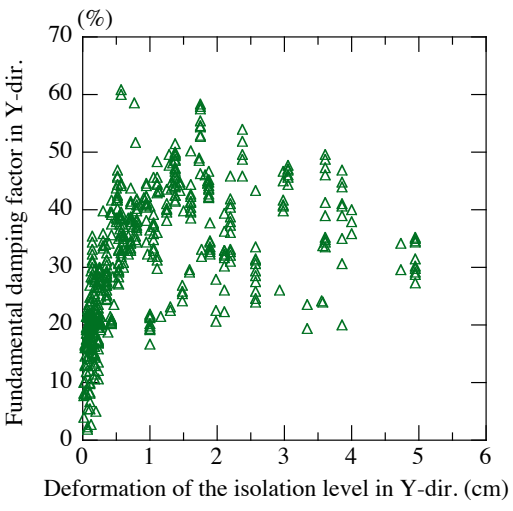

(e) Relationship between deformation of the isolation level and fundamental damping factor in Y-dir.

Fig. 6 – Variations of dynamic characteristics of CSI building in Y direction

5. Effects of CSI System from Long-term SHM

5.1 Effects of CSI system from 231 Earthquakes

The SHM system of the Safety and Security Center (Fig. 3) records seismic vibrations when the observed acceleration of any accelerometer in any direction exceeds 3 cm/s^2 RMS for more than 1 s. Furthermore, the control system unlocks the fluid dampers when the observed ground motion exceeds 5 cm/s^2 RMS for more than 1 s in the horizontal direction, or 8 cm/s^2 RMS for more than 1 s in the vertical direction. The SHM system has recorded 231 earthquake motions since 2006, including the 2011-TPE.

Fig. 7 shows the amplification characteristics of the core structure relative to the ground level. The observed peak acceleration $a_{max}^{Top-core}$ on the top of the core structure is amplified up to six times as compared with a_{max}^{Ground} on the ground level. The amplification factor $a_{max}^{Top-core}/a_{max}^{Ground}$ varies widely and has almost no relation to a_{max}^{Ground} or the locked/released condition of the fluid dampers.

Fig. 8 shows the isolation effects of the CSI mechanism that consists of two layers each of four inclined rubber bearings. The amplification factor is obtained as the ratio of the observed peak acceleration $a_{max}^{Upper-isolator}$ on the upper isolator to $a_{max}^{Top-core}$ on the top of the core structure. The amplification factors $a_{max}^{Upper-isolator}/a_{max}^{Top-core}$ clearly decreases with $a_{max}^{Top-core}$ and falls below unity for $a_{max}^{Top-core} > 10$ cm/s^2 and below a half for $a_{max}^{Top-core} > 30$ cm/s^2, which reveals the isolation effect of the CSI mechanism. Note that this isolation effect is unaffected by the locked/released condition of the fluid dampers.

Fig. 9 shows the SI effects on the second floor in the CSI building relative to the ground level. The other amplification factor is obtained as the ratio of the observed peak acceleration $a_{max}^{2nd-floor}$ on the second floor to a_{max}^{Ground} on the ground level. The amplification factor $a_{max}^{2nd-floor}/a_{max}^{Ground}$ decreases with a_{max}^{Ground} and falls below unity for $a_{max}^{Ground} > 10$ cm/s^2, which is when the locks of the fluid dampers are released. Fig. 9 shows that the CSI system brings about the SI effect of reducing the response acceleration of the suspended structure by roughly half for $a_{max}^{Ground} > 30$ cm/s^2.

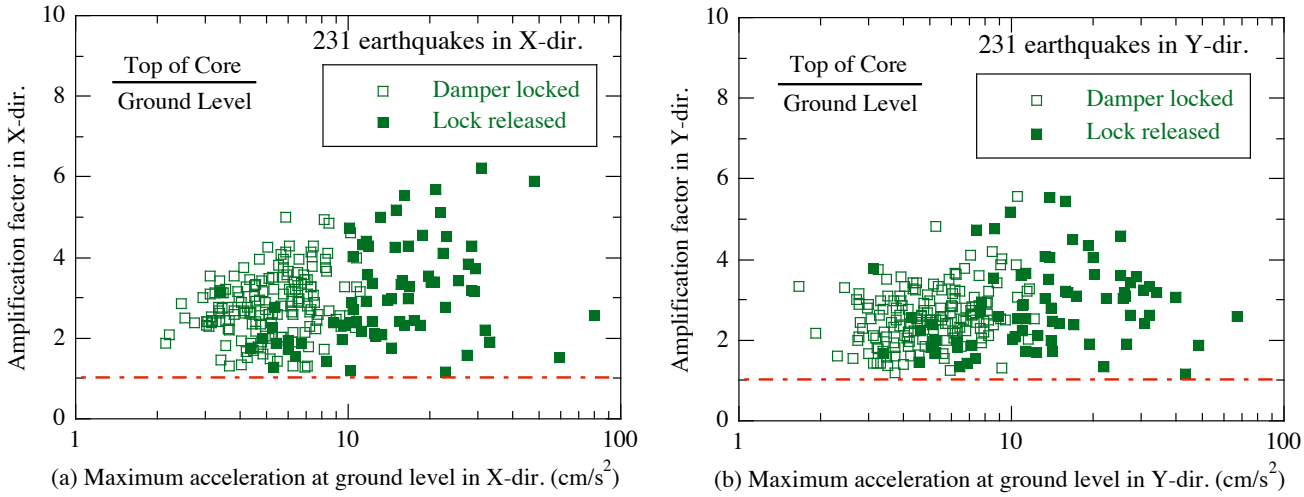

(a) Maximum acceleration at ground level in X-dir. (cm/s^2)

(b) Maximum acceleration at ground level in Y-dir. (cm/s^2)

Fig. 7 – Amplification characteristics of core structure relative to ground level

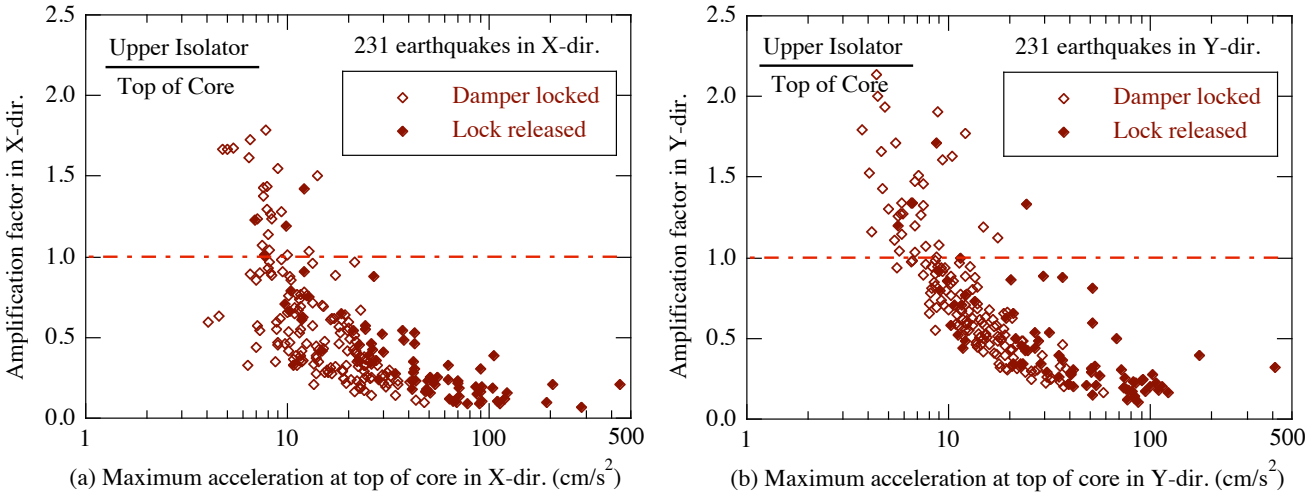

Fig. 8 – SI effects of CSI mechanism comprising two layers each of four inclined rubber bearings

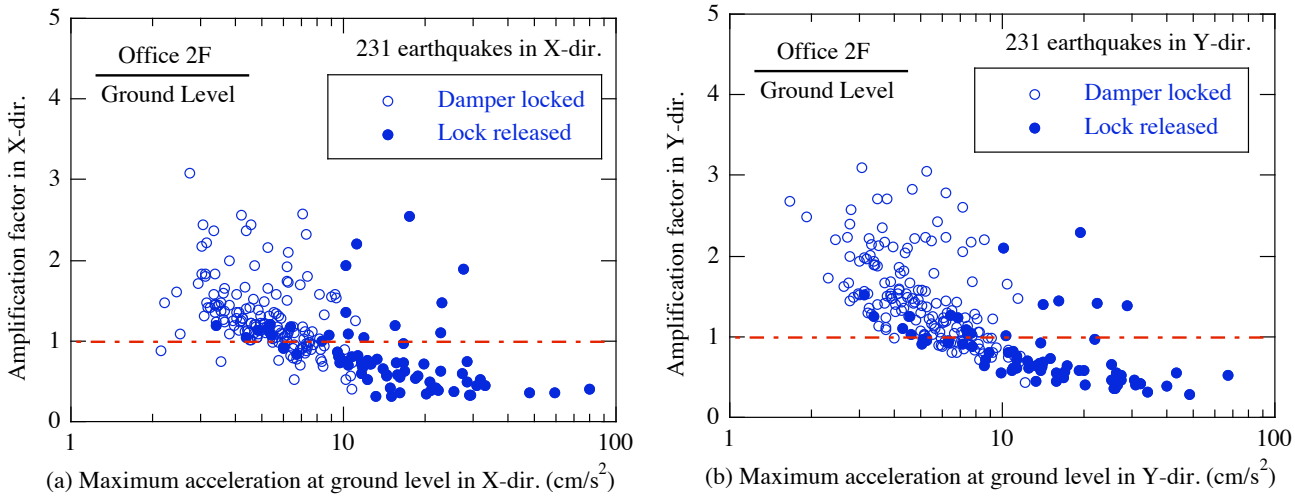

Fig. 9 – SI effects on second floor of CSI building relative to ground level

5.2 Dynamic Characteristics from Daily Microtremor Measurements

The SHM system has also been collecting a 2-min microtremor trace at midnight each day since December 2006. Fig. 10 shows the estimated fundamental frequencies in the horizontal X and Y directions for 3898 days when the fluid dampers were locked. The fundamental frequency in each direction remained almost constant over the observation period, exhibiting no distinct change after the 2011-TPE. These results imply that the building suffered no structural damage from the 231 observed earthquake events including the 2011-TPE.

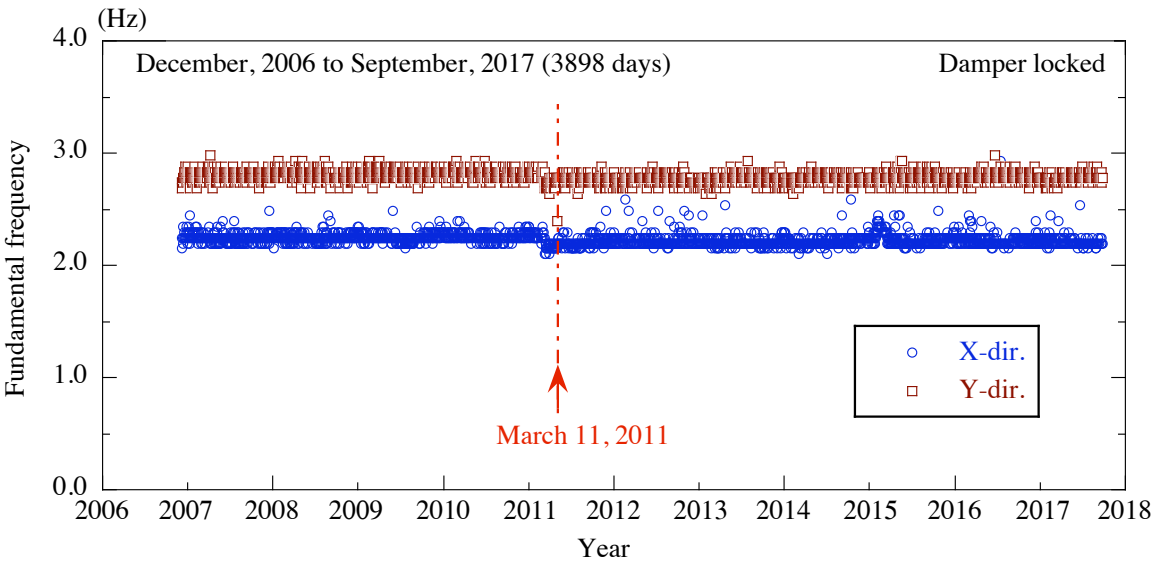

Fig. 10 – Variations of fundamental frequency estimated from daily microtremor measurements

6. Conclusions

The Safety and Security Center in Tokyo, Japan was the first building to use the CSI system. The SI mechanism for the building comprises two layers each of four inclined rubber bearings installed at the top of a reinforced concrete core, from which three floors of office structure are suspended by high-strength steel rods. Fluid dampers with a safety locking mechanism are installed between the core shaft and the suspended office structure at the second floor and rooftop levels. An SHM system was installed in the Safety and Security Center and has detected and recorded 231 earthquake motions since 2006, including the 2011-TPE, and has been collecting a 2-min microtremor trace each day.

The 2011-TPE revealed the effect of the CSI system of the building. Compared with the maximum acceleration on the ground, the CSI system reduced those on the floors in the suspended structure to roughly a half in the X direction and a third in the Y direction. The temporal changes of the fundamental period and damping factor during the 2011-TPE were estimated based on an ARX model by assigning the wave on the ground level as the input and the two waves on the office rooftop and on the office second floor as two outputs in each horizontal direction. The fundamental period increases with the deformation of the isolation level, while the fundamental damping factor is related only weakly to that deformation.

The 231 observed earthquake records reveal the SI features of the CSI system. The CSI two-layered isolator can reduce the peak acceleration on the upper isolator by half compared to the one on the top of the core structure for over 30 cm/s^2, irrespective of the locked/released condition of the fluid dampers. The CSI system realizes the SI effect of reducing the response acceleration of the suspended structure to roughly half for the peak ground acceleration over 30 cm/s^2.

The 3898 days of daily microtremor measurements enable any building damage due to earthquakes to be diagonosed. The fundamental frequencies in the horizontal X and Y directions remain almost constant over the observation period and show no distinct change after the 2011-TPE. These results imply that the building suffered no structural damage from the 231 observed earthquake events including the 2011-TPE.

The CSI system has been developed as an utterly new type of SI system. The SHM system installed in the Safety and Security Center has revealed the dynamic properties of the building and shown the effectiveness of the CSI system at reducing the response acceleration of the suspended structure. These results can help future developments and applications of the CSI system.

7. Acknowledgements

The present CSI system was studied in joint research between Tokyo Institute of Technology, Ove Arup & Partners (Tokyo), Daiichi-Kobo Associates, and Shimizu Corporation. The authors would like to thank Prof. Akira Wada, Prof. Toru Takeuchi, Mr. Shigeru Hikone, and Mr. Teiichi Takahashi for their collaboration in developing the CSI system.

8. References

[1] Nakamura Y, Saruta M, Nakanishi T, Wada A, Takeuchi T, Hikone S, Takahashi T (2008): Development of the core-suspended isolation system. *Proceedings of the 14th World Conference on Earthquake Engineering*, Beijing, China.

[2] Nakamura Y, Saruta M, Wada A, Takeuchi T, Hikone S, Takahashi T (2011): Development of the core-suspended isolation system. *Earthquake Engineering & Structural Dynamics,* 40(4), 429-447. doi:10.1002/eqe.1036.

[3] Anderson P (1985): Adaptive forgetting in recursive identification through multiple models. *International Journal of Control*, 42(5), 1175-1193.

[4] Ljung L (1987): *System Identification*. Prentice Hall.

[5] Şafak E (1989): Adaptive modeling, identification, and control of dynamic structural systems. I: Theory & II: Applications. *Journal of Engineering Mechanics,* 115, 2386-2405 & 2406-2426.

[6] Çelebi M, Şafak E (1991): Seismic response of Transamerica Building. I: Data and Analysis & II: System Identification. *Journal of Structural Engineering*, 117(8), 2389-2425.

[7] Şafak E (1991): Identification of linear structures using discrete-time filters. *Journal of Structural Engineering,* 117(10), 3064-3085.

[8] Çelebi M, Şafak E(1992): Seismic response of Pacific Park Plaza. I: Data and Preliminary Analysis & II: System Identification. *Journal of Structural Engineering*, 118(6), 1547-1589.

[9] Çelebi M (1993): Dynamic characteristics of five tall buildings during strong and low-amplitude motions. *The Structural Design of Tall Buildings*, 2, 1-15.

[10] Şafak E. (1993). Response of a 42-storey steel-frame building to the M_s=7.1 Loma Prieta earthquake. *Engineering Structures*, 15(6), 403-421.

[11] Saito T, Okada K, Yokota H (1994): System identification of steel frame buildings through observed earthquake records. Part I and II. *Summaries of technical papers of Annual Meeting, Architectural Institute of Japan*, 673-676. (in Japanese)

[12] Okada K, Yokota H (1994): Dynamic characteristics of steel frame buildings using system identification technique, *Proceedings of the 9th Japan Earthquake Engineering Symposium*, 1717-1722, Tokyo, Japan. (in Japanese)

[13] Loh C, Tou I (1995): A system identification approach to the detection of changes in both linear and non-linear structural parameters. *Earthquake Engineering & Structural Dynamics*, 24(1), 85-97.

[14] Loh, C, Lin H (1996): Application of off-line and on-line identification techniques to building seismic response data. *Earthquake Engineering & Structural Dynamics*, 25(3), 269-290.

[15] Saito T, Yokota H (1996): Evaluation of dynamic characteristics of high-rise buildings using system identification techniques. *Journal of Wind Engineering & Industrial Aerodynamics*, 59(2-3)21, 299-307.

[16] Saito T (1998): System identification of a high-rise building applying multi-input-output ARX model of modal analysis. *Journal of Structural and Construction Engineering, Architectural Institute of Japan*, 508, 47-54. (in Japanese)

[17] Ikeda Y, Hisada Y (2013): Earthquake responses on all floors in a building estimated by observation records on some restricted floors. *Journal of Japan Earthquake Engineering*, 13(4), 38-54. (in Japanese)

[18] Siringoringo DM, Fujino Y (2015): Long-term seismic monitoring of base-isolated building with emphasis on serviceability assessment, *Earthquake Engineering & Structural Dynamics*, 44(4), 637-655. doi:10.1002/eqe.2538.

[19] Okada K, Shiraishi M, Iwaki H, Shiba K (2003): Internet-based remote controlled structure monitoring system. *Structural Health Monitoring and Intelligent Infrastructure*. *Proceedings of the First International Conference SHMII-01*, Tokyo, Japan.

[20] Okada K, Nakamura Y, Saruta M (2009): Application of earthquake early warning system to seismic-isolated buildings. *Journal of Disaster Research*,4, 570-578. doi:10.20965/jdr.2009.p0242.

[21] Okada K, Kataoka S (2016): Overall building response estimation method on records from two seismographs. *The Journal of Japan Association for Earthquake Engineering*, 16, 94-113.

[22] Nakamura Y, Hanzawa T, Hasebe M, Okada K, Kaneko M, Saruta M (2011): Report on the seismic isolation methods from the 2011 Tohoku-Pacific Earthquake. *Seismic Isolation and Protection Systems*, 2, 57-74.

[23] Tomizawa T, Takahashi O, Suhara J, Okada K, Tsuyuki Y, Fujita T (2012): A study on earthquake observation record in the building using the three-dimensional seismic isolation system. *Journal of Structural and Construction Engineering, Architectural Institute of Japan*, 679, 1393-1402. (in Japanese)

[24] Yoshimoto R, Mita A, Okada K (2005): Damage detection of base-isolated buildings using multi-input multi-output subspace identification. *Earthquake Engineering & Structural Dynamics*, 34, 307-324. doi:10.1002/eqe.435.

